RESEARCH ARTICLE

International Journal of QUANTUM CHEMISTRY WILEY

Si_6C_{18}: A bispentalene derivative with two planar tetracoordinate carbons

Diego Inostroza[1,2] | Luis Leyva-Parra[1,2] | Osvaldo Yañez[3,4] | J. César Cruz[5] | Jorge Garza[5] | Víctor García[6] | Venkatesan S. Thimmakondu[7] | Maria L. Ceron[8] | William Tiznado[1]

[1]Computational and Theoretical Chemistry Group, Departamento de Ciencias Química, Facultad de Ciencias Exactas, Universidad Andres Bello, Santiago, Chile

[2]Programa de Doctorado en Fisicoquímica Molecular, Facultad de Ciencias Exactas, Universidad Andres Bello, Santiago, Chile

[3]Center of New Drugs for Hypertension (CENDHY), Santiago, Chile

[4]Facultad de Ingeniería y Negocios, Universidad de las Américas, Santiago, Chile

[5]Departamento de Química, División de Ciencias Básicas e Ingeniería, Universidad Autónoma Metropolitana-Iztapalapa, Ciudad de México, Mexico

[6]Facultad de Química e Ingeniería Química, Universidad Nacional Mayor de San Marcos, Lima, Peru

[7]Department of Chemistry and Biochemistry, San Diego State University, San Diego, California, USA

[8]Facultad de Ingeniería, Universidad Finis Terrae, Santiago, Chile

Correspondence
Luis Leyva-Parra and William Tiznado, Computational and Theoretical Chemistry Group, Departamento de Ciencias Química, Facultad de Ciencias Exactas, Universidad Andres Bello, República 275, Santiago, Chile.
Email: wtiznado@unab.cl and l.leyvaparra@uandresbello.edu

Abstract

Here we show that substituting the ten protons in the dianion of a bispentalene derivative ($C_{18}H_{10}^{2-}$) by six Si^{2+} dications produces a minimum energy structure with two planar tetracoordinate carbons (ptC). In Si_6C_{18}, the ptCs are embedded in the terminal C_5 pentagonal rings and participate in a three-center, two-electron (3c-2e) Si-ptC-Si σ-bond. Our exploration of the potential energy surface identifies a triphenylene derivative as the putative global minimum. Nevertheless, robustness to Born–Oppenheimer molecular dynamics (BOMD) simulations at 900 and 1500 K supports bispentalene derivative kinetic stability. Chemical bonding analysis reveals ten delocalized π-bonds, which, according to Hückel's $4n + 2$ π-electron rule, would classify it as an aromatic system. Magnetically induced current density analysis reveals the presence of intense local paratropic currents and a weakly global diatropic current, the latter agreeing with the possible global aromatic character of this specie.

KEYWORDS
chemical bonding analysis, DFT computations, global minimum, planar tetracoordinate carbon, silicon-carbon clusters

1 | INTRODUCTION

Nowadays, molecules or clusters with planar hypercoordinate carbon (phC) are no longer a curiosity, given the experimental and theoretical effort to synthesize or design systems with these features [1–5]. The phCs isolation and experimental characterization initially seemed not feasible because they do not meet the apparent structural consequence of tetrahedral geometry in a tetracoordinate carbon, that is, they violate the van't Hoff and Le Bel principle. The pioneers to point out how to stabilize these systems was Monkhorst (1968), who evaluated the stereomutation of
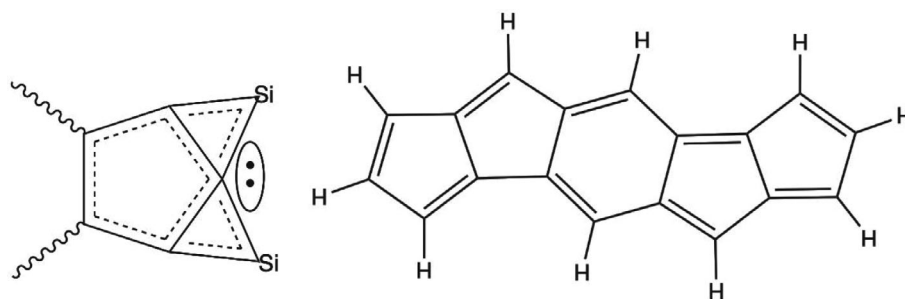
SCHEME 1   On the left is a representation of how ptCs are formed by replacing 3 H^+ with 2 Si^{2+} on a C_5 ring [4, 22, 29]. On the right is the bispentalene derivative used as a molecular template in this work.

methane theoretically through a planar tetracoordinate carbon (ptC) transition state [6]. Two years later, Hoffmann and co-workers proposed different approaches to stabilize a ptC to achieve a thermally accessible transition state for a racemization process [7].

Remarkable progress has been made in the chemistry of phCs in the last 50 years. Several experimentally identified systems have been reported, and others proposed "in silico" with experimental feasibility, given their thermodynamic and (or) kinetic stability [1–3, 8–13]. The most recent findings concern higher coordination with reported systems that exhibit planar penta- [14–23] and hexacoordinate carbons [24–27]. An important, though not indispensable, factor in the stabilization of many of these systems is the presence of delocalized bonds, which is why the concept of aromaticity is frequently invoked to explain stability [4, 7, 22, 28].

Inspired by Hoffman and co-workers' ideas on electronic stabilization to achieve ptCs, some of us proposed a strategy to design ptC global minima (GM). The strategy replaced protons from an aromatic hydrocarbon with E^{2+} dications (E = Si—Pb) [5]. In this way, the preservation of the π-aromatic circuits of the parent aromatic hydrocarbons is ensured. This strategy has been initially tested on derivatives of the cyclopentadienyl anion ($C_5H_5^-$) and the pentalene dianion ($C_8H_6^{2-}$). Some GM resulting structures were obtained: Si_3C_5, Ge_3C_5, Si_4C_8, and Ge_4C_8, containing one or two ptCs. A striking feature of these clusters is that they are globally π-aromatic and possess three-center, two-electron (3c-2e) E-ptC-E σ-bonds (local σ-aromaticity). More recently, we have shown that whenever there is the possibility of forming a C_5 ring bridged with at least two Si in small C—Si clusters (Si_nC_n; n = 5, 8, and 9), aromaticity and ptCs in the GM structures are evidenced (see Scheme 1) [29]. Besides, there are other aromatic hydrocarbon derivatives with ptCs; however, all stem from small cyclic hydrocarbons [4, 22, 30, 31]. Also, recent work has shown that combining carbon with heavier group 14 elements is a successful approach to obtaining ptCs [32–34].

This work reports a study that challenges the design rule described above in a larger C—Si compound. We have identified a polycyclic hydrocarbon containing C_5 rings, a bispentalene derivative, a simplified model of a compound synthesized and characterized by Cao et al. in 2015, where hydrogens have replaced the bulky substituents linked to the carbons of the polycyclic circuit [35]. The polycyclic circuit has 18 π-electrons, that is, it complies with Hückel's [$4n + 2$] π-electron rule. The aromatic character of this species has been a matter of controversy; initially, it was assumed the manifestation of a paratropic (antiaromatic) global ring current and a diatropic (aromatic) local ring current (around the benzene ring) in the presence of an external magnetic field. This analysis was based on the calculations of the nucleus-independent chemical shift (NICS)-XY-scan [35]. However, a more recent study analyzing the ring currents explicitly, concludes that the compound is globally non-aromatic, while the local and semi-local rings (pentalenes) are antiaromatic [36]. The NICS limitations to describe aromaticity in this system agree with the other evidence on the coupling of local and global contributions to NICS [37–42], which prevents us from correctly establishing the different ring current circuits and their intensities in a polycyclic system. However, aromaticity is not uniquely defined; using different aromaticity-based criteria is advisable to have a more detailed description of aromaticity [43, 44].

Our density functional theory (DFT) calculations show that the design ptC-Si_6C_{18} system is a local minimum on its potential energy surface (PES). Furthermore, our molecular dynamics simulations support the dynamic persistence of this structure, even at high temperatures (900 and 1500 K). This suggests that the ptC-Si_6C_{18} system, with two ptC units, is kinetically viable. However, our PES exploration reveals a better minimum, corresponding to a triphenylene derivative. These results evidence the importance of analyzing kinetic and thermodynamic stability in studying atomic clusters to provide insight into their experimental feasibility, at least in gas-phase experiments.

2 | COMPUTATIONAL DETAILS

The PES of the title cluster has been explored using the AUTOMATON program [45, 46]. In addition, the search has been complemented by substituting and permutations of atoms until reaching the formula Si_6C_{18} from different molecular templates (see details in Figure S1). Besides, the best structures of these searches were checked, and new candidates were generated manually by permuting Si positions by C. The lowest energy structures have been checked, and some additional atomic permutations have been performed manually [47, 48]. Geometric optimizations

were performed at the PBE0 [49]/SDDALL [50] level in the search process, and at the PBE0-D3 [51]/Def2-TZVP [52] level, the best structures were refined. The vibrational frequencies were evaluated simultaneously to confirm the optimized structures as true minima on the PES. These calculations were performed using the Gaussian16 program [53].

The current densities were computed using the GIMIC program [54, 55] which employs the gauge included atomic orbital (GIAO) method [56] at the PBE0-D3/Def2-TZVP level. These calculations consider an external magnetic field perpendicularly directed to the molecular plane. In our analysis, diatropic (aromatic) and paratropic (antiaromatic) ring currents circulate clockwise and counterclockwise. To visualize the currents, we used Paraview 5.10.0 software [57, 58]. The ring current strength (RCS) was obtained after considering different rectangular integration planes, intersecting the selected bonds, and with a starting point in the center of rings of interest (see Figures S2 and S3). For integration, GIMIC uses the two-dimensional Gauss-Lobatto algorithm [55, 59]. Positive/negative RCS values characterize diatropic (aromatic)/patratropic (anti-aromatic) ring currents. In addition, values close to zero suggest a non-aromatic character [60].

Chemical bonding is analyzed by different methods: Wiberg bond indices (WBI) [61], natural population analysis (NPA) [62], and the adaptive natural density partitioning method (AdNDP) [63, 64]. These approaches are based on the natural bond orbital (NBO) method and were performed using the wavefunction obtained at the PBE0-D3/Def2-TZVP level. The WBI and NPA were calculated with the NBO 6.0 code [65], the AdNDP analysis was performed using Multiwfn 3.8 [66]. The molecular structures and AdNDP orbitals were visualized with CYLview 2.0 [67] and VMD 1.9.3 [68]. The dynamic behavior was assessed through Born Oppenheimer molecular dynamics (BOMD) simulations [69] on graphics processing units (GPUs) at the PBE0-D3/6-31g* level. The BOMD simulations involve 50 ps (with a time step of 0.5 fs) at 900 and 1500 K and within the NVT ensemble. The rate-rescaling thermostat was applied to keep the system temperature constant. The calculations were performed with the quantum chemistry package TeraChem [70].

3 | RESULTS AND DISCUSSION

The design rule to be challenged in this work was tested in aromatic hydrocarbons with pentagonal rings [4, 5, 22, 29, 71]. The $C_{18}H_{10}$ polycycle system is globally non-aromatic and locally antiaromatic. Therefore, we have added two electrons in the $C_{18}H_{10}^{2-}$ dianion to promote aromaticity. $C_{18}H_{10}^{2-}$, which is a local minimum, exhibits a weak global aromatic character but retains the local antiaromaticity of the neutral system. Figure 1 shows a schematic representation of the detected ring currents, following a previously proposed methodology [36, 41, 60, 72], by analyzing the profiles of different integration planes (see Figure S3). As shown, $C_{18}H_{10}^{2-}$, with 20 π-electrons, evidence a global diatropic current on the periphery of the polycycle, with an RCS of 7.0 nA T^{-1}, and a marginal global paratropic current (RCS = −1.2 nA T^{-1}), resulting in a weakly diatropic global current (RCS = 5.8 nA T^{-1}). Consider that benzene (C_6H_6) has a net RCS of 11.8 nA T^{-1}. This analysis suggests that although $C_{18}H_{10}^{2-}$ comes from a reduction of an experimentally viable system and complies with having pentagonal rings, it does not fully comply with the aromaticity criterion since its global aromatic character counters with its strong local antiaromatic character. It, therefore, emerges as a suitable system to evaluate the importance of π-aromaticity in the parent hydrocarbon for the viability of the designed Si-C system (with ptCs).
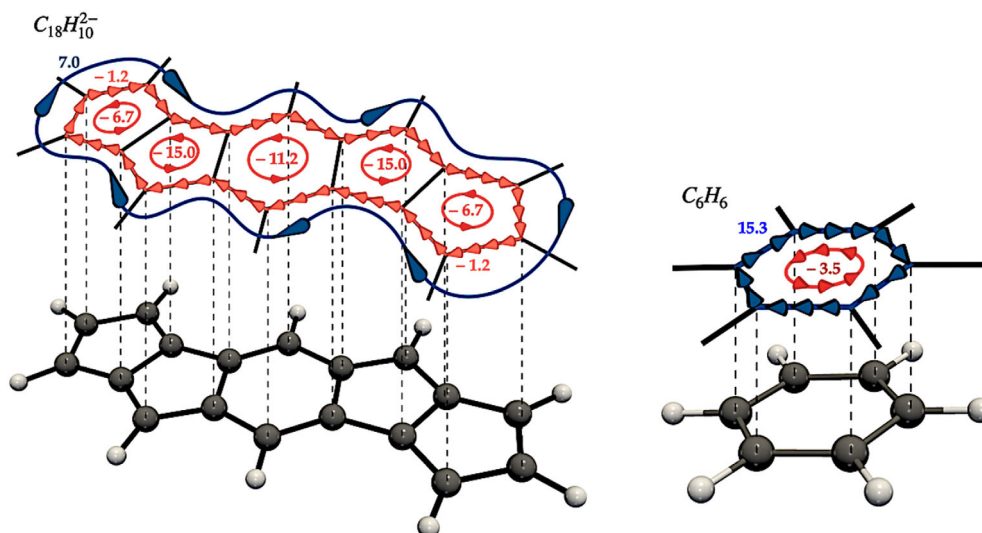

FIGURE 1 Schematic representation of the ring currents of $C_{18}H_{10}^{2-}$ (left) and C_6H_6 (right) for comparison. The numbers represent the RCS values of each ring's current path in nA T^{-1}

What happens when replacing the ten H^+ of $C_{18}H_{10}^{2-}$ with six Si^{2+}? We achieve a minimum on the PES (to verify whether it is the GM) with two ptCs (ptC-Si_6C_{18}) where the C_{18} polycycle shape of the parent hydrocarbon persists. The first concern regarding ptC-Si_6C_{18} is its aromatic character. Figure 2 shows the ring currents circuits detected in this system and their strength (RCSs). We can appreciate variations concerning $C_{18}H_{10}^{2-}$; now, the global diatropic current (in the periphery of the whole system) is less intense (4.8 nA T^{-1}). Also emerge local diatropic currents around the C_5 rings at the ends (4.4 nA T^{-1}) and a weak semilocal paratropic ring current surrounding the central tricycle (3.3 nA T^{-1}). The local paratropic ring currents decrease in strength (-5.0 to -9.7 nA T^{-1}) regarding the values of -8.7 to -15.0 nA T^{-1} in Si_6C_{18}. Interestingly, a local ring current is also evident inside the Si-ptC-Si moiety, which has been a repeating pattern in these ptC species and is a consequence of a multi-centric 3c-2e σ-bond in this fragment, as will be discussed in detail below.

Figure 3 shows the chemical bonding interpretation for the ptC-Si_6C_{18} cluster according to AdNDP analysis. There are six lone pairs (one on each Si), and 22 2c-2e C—C σ-bonds connecting the C_{18} polycycle. Each of the two ptCs is connected to two Si through 3c-2e Si-ptC-Si σ-bonds, a feature highlighted as local aromaticity and stabilizing factor in these species [4, 5, 7, 22]. Eight 2c-2e Si—C σ-bonds connect the Si's to the C_{18} polycycle through bridging bonds on the C—C edges. AdNDP also recovered a set of 10 π-delocalized bonds distributed on the complete planar system, suggesting the possibility of aromaticity according to Hückel's rule. However, this contrasts with the current density analysis, highlighting the limitation of this rule, especially in polycyclic systems, where electrons are distributed between local, semi-local, or global circuits. This chemical bonding picture entirely agrees with the WBI analysis (Figure S4). The C—C bonds of the polycycle have WBI values intermediate between single and double bonds (1.2–1.4), and the bridged C—Si have close to single bond WBI values (0.7–1.0), except those connecting to ptC, where the WBI_{C-Si} is 0.54, in agreement with the 3c-2e Si-ptC-Si σ-bond detected by AdNDP. The NPA charges are positive on the Si ($\sim 1.0 |e|$) and negative on the C's bonded to these Si, agreeing with the electronegativity difference between these atoms. WBI and NPA calculations have also been performed at the MP2/aug-cc-pVTZ [73–76]//PBE0-D3/aug-cc-pVTZ level to support the reliability of the calculations. Figure S4 shows minimal changes on these properties and does not alter the conclusions.

The bonding analysis reveals a significant C—C and C—Si covalent bonding character in the ptC-Si_6C_{18} system, suggesting a structural persistence, that is, resistance to isomerization, which would account for its kinetic stability. The latter is confirmed by our molecular dynamic simulations, where it is shown that even at high temperatures (900 and 1500 K) the structure persists throughout the simulation time (50 ps). In the supporting material, we report two small movies with these dynamics, showing that there are reversible movements of
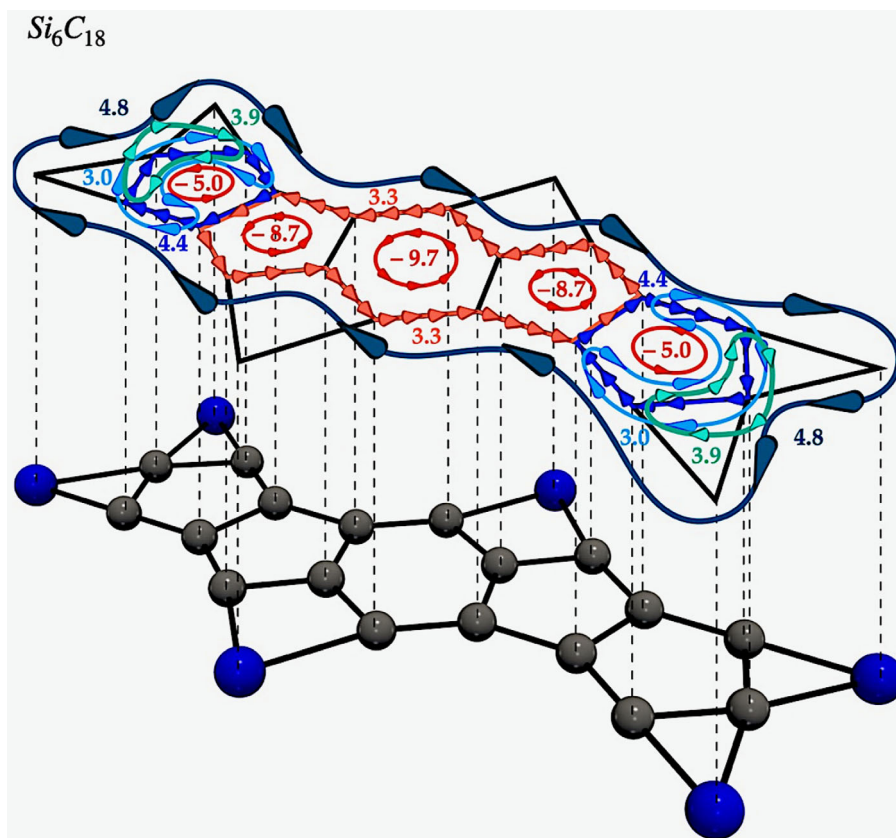

FIGURE 2 Schematic representation of the ring currents of ptC-Si_6C_{18}. The numbers represent the RCS values of each ring's current path in nA T^{-1}
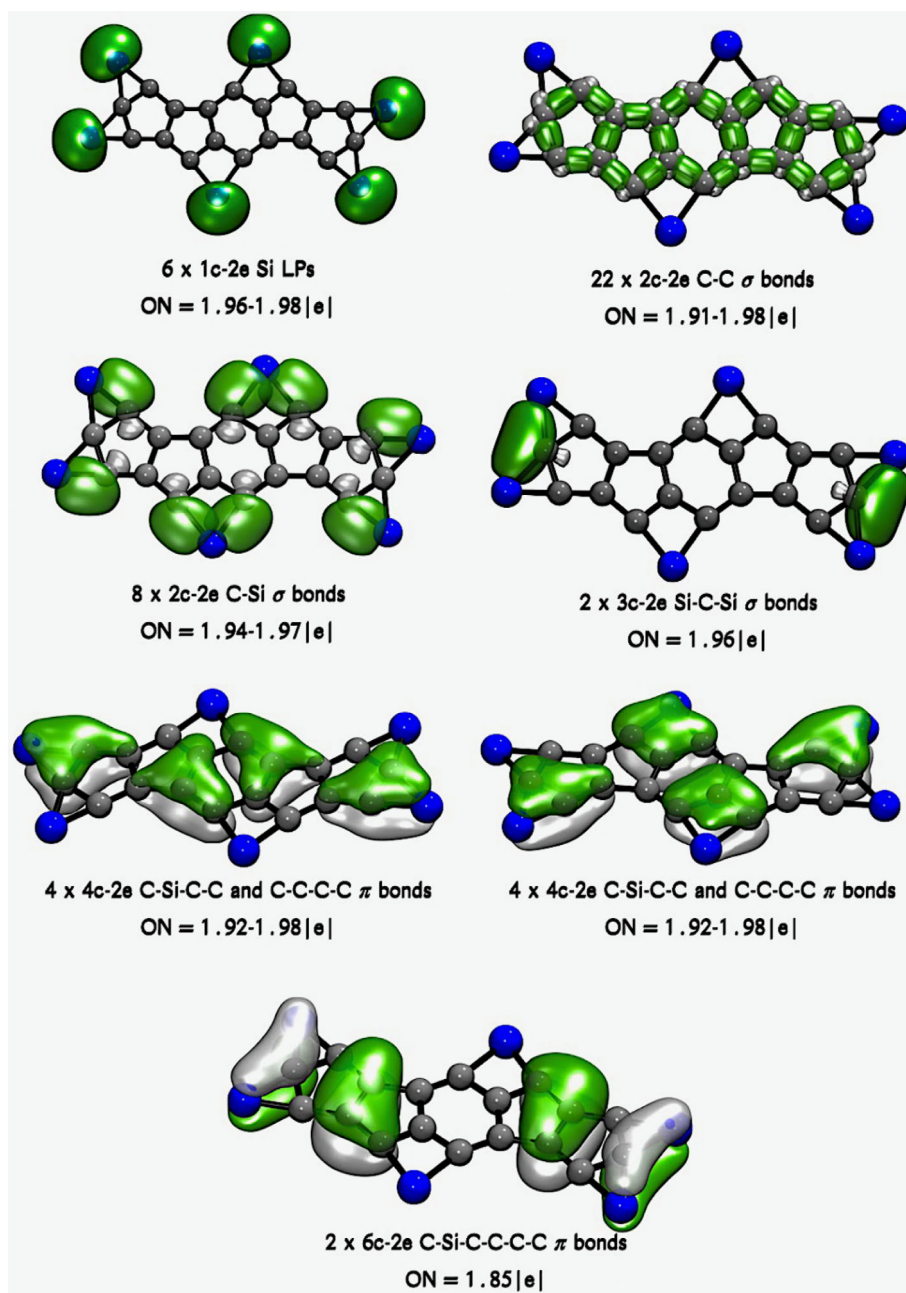
FIGURE 3 AdNDP bonding pattern of ptCs-Si_6C_{18} cluster. Occupation numbers (ONs) are shown

the atoms during the dynamics. The structural fluctuations are represented by the root mean squared deviations curve (RMSD, in Å) versus simulation time (Figure 4). The two RMSD show important oscillations (in agreement with the high temperatures) but reversible, such as what is observed in the movies. This implies that the basic structure persists during the simulation, demonstrating its rigidity at these high temperatures.

Up to this point of the discussion, we are sure about the kinetic stability of ptC-Si_6C_{18}, that is, its persistence to isomerization. However, it remains to be answered whether it corresponds to GM. To answer this, we have performed an exploration of the PES from different approaches, as described in the computational details. Figure 5 reports the best minima identified for the Si_6C_{18} combination (at the PBE0-D3/Def2-TZVP level), the Cartesian coordinates of which are shown in Table S1 of the Supplementary Material. The best minima, including the putative GM, are in the singlet state. The lowest energy triplet is 15.6 kcal mol^{-1} above the putative GM. This search reveals that ptC-Si_6C_{18} is the fourth isomer (**4**) lying 70.4 kcal mol^{-1} above the putative GM (**1**), **1** is a triphenylene derivative. Interestingly, the PES screening identifies the isomer **3** (at 65.7 kcal mol^{-1}), which has three ptCs, highlighting how frequent the formation of ptCs is if carbon polycycles with five-membered rings are favored.
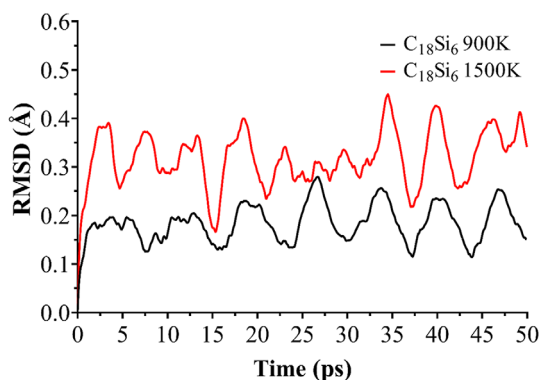
FIGURE 4 RMSD versus time in the BOMD simulations of ptC-Si_6C_{18} at 900, and 1500 K
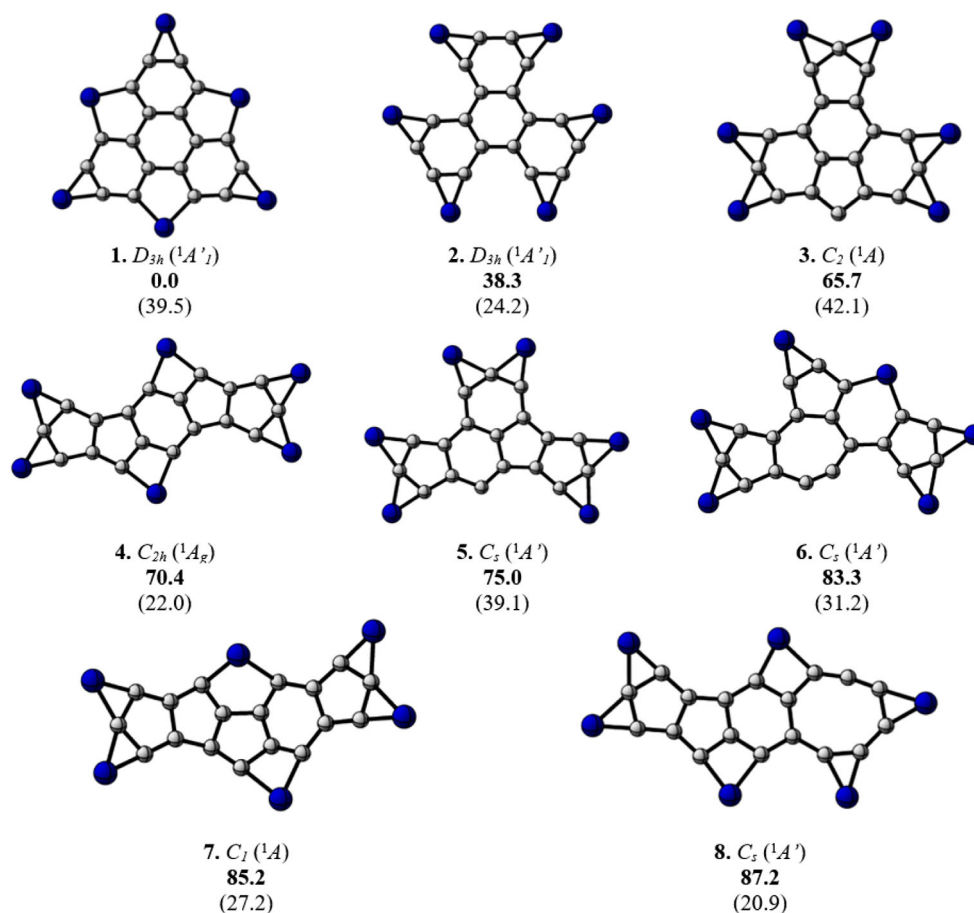

FIGURE 5 Lowest energy-optimized structures of Si_6C_{18}, their point group symmetries, and spectroscopic states. The relative energies at the PBE0-D3/Def2-TZVP level including ZPE (ZPE = zero-point corrected) and the lowest frequency at the same level in bold and parenthesis (in cm^{-1}), respectively, are also reported. A number-letter label identifies structure to facilitates their connection with their Cartesian coordinates (in the ESI)

For comparative purposes, the best structures have also been optimized at the ωB97X-D [77]/Def2-TZVP level (the ωB97X-D functional includes an explicit empirical dispersion correction), noting minor differences in the relative energies (see Table S2). However, the order of the isomers is maintained.

Therefore, ptC-Si_6C_{18} is a kinetically stable local minimum but not the GM structure. These results highlight the importance of exploring the PES in studies where a new system is proposed to support its feasibility in gas-phase experiments. In this case, starting from a classical molecule with evidence of its synthesis and experimental characterization led us to design a kinetically viable species. However, the exploration of its PES
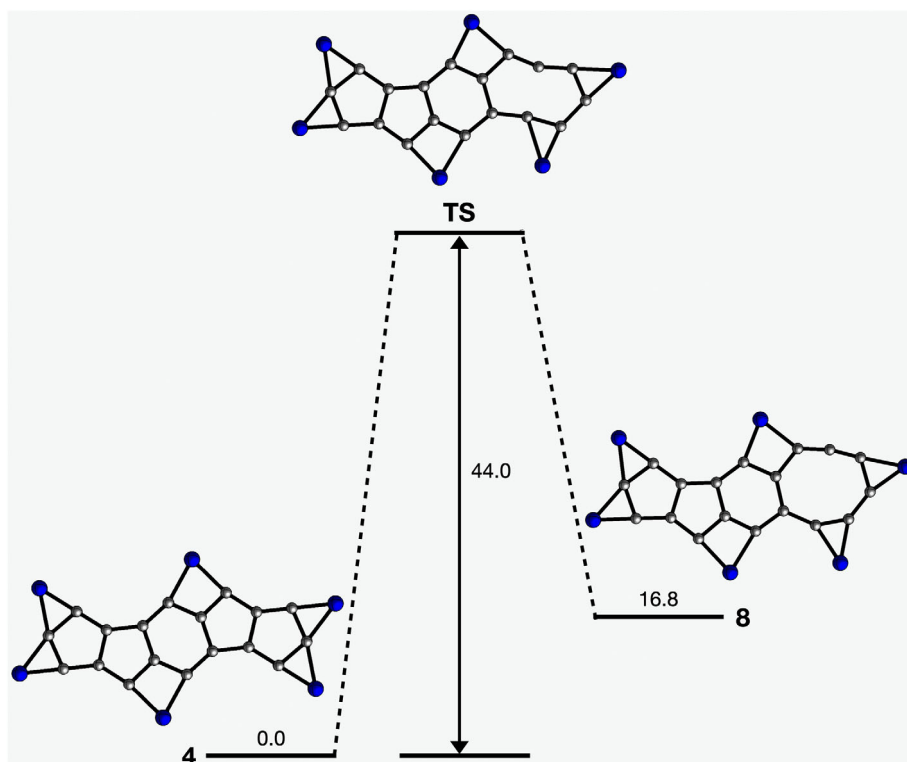
FIGURE 6 Energy profile for the isomerization of **4** to **8** at PBE0-D3/Def2-TZVP including ZPE (ZPE = zero-point corrected). The energies are given in kcal mol^{-1}

indicates that it does not correspond to the GM. Therefore, its experimental feasibility would depend on favoring the formation of this structure, which, once formed, is stable enough to avoid isomerization. In other words, the transformation of isomer 4 into more stable isomers would have to occur through several steps, which include peripheral silicon displacements and C—C bond cleavages. To illustrate this, we have calculated that the barrier for isomerization from **4** to **8** (Figure 6) is prohibitively high, 42.7 kcal mol^{-1} at the PBE0-D3/Def2-TZVP level. For 4 to transform to **1**, the pentagonal rings must inevitably open (maybe through isomer **8**). Therefore, this simulation, in conjunction with the BOMD simulations, supports our point about the kinetic stability of **4**.

4 | CONCLUSIONS

The ptC-Si_6C_{18} species has been designed as a derivative of a bispentalene dianion ($C_{18}H_{10}^{2-}$), whose neutral species has been synthesized and experimentally characterized. The ptC-Si_6C_{18}, with two ptCs, is a local minimum on the PES. Magnetically induced current density analysis suggests that this species is globally weakly aromatic. However, this contrasts with its strong semilocal and local antiaromatic character. Chemical bonding analysis detects 10 delocalized π-bonds distributed throughout the system, fulfilling Hückel's $4n + 2$ rule for aromatic systems. However, since it is a polycyclic system, the bonds are local, semilocal, and globally delocalized, making this rule limited for inferring aromaticity. The bonding analysis also detects a delocalized 3c-2e σ-bond in the Si-ptC-Si fragments, which is a feature in these derivatives and consistent with seeing a local diatropic ring current in this region.

The structure of the ptC-Si_6C_{18} system proves to be persistent upon molecular dynamics simulations at high temperatures (900 and 1500 K), suggesting high kinetic stability. Therefore, ptC-Si_6C_{18} would be viable only if the conditions for its formation are favored because the barriers to isomerize towards the GM are high enough.

AUTHOR CONTRIBUTIONS

Diego Inostroza: Conceptualization; methodology; software; validation; writing – review and editing. **Osvaldo Yañez:** Investigation; methodology; validation; writing – review and editing. **J. César Cruz:** Methodology; software; validation; writing – review and editing. **Jorge Garza:** Formal analysis; funding acquisition; software; supervision; writing – review and editing. **Víctor García:** Investigation; methodology; software; visualization; writing – review and editing. **Venkatesan S. Thimmakondu:** Formal analysis; investigation; methodology; resources; software; validation; writing –

DATA AVAILABILITY STATEMENT

The data that supports the findings of this study are available in the supplementary material of this article.

ORCID

J. César Cruz https://orcid.org/0000-0002-3608-1733

Venkatesan S. Thimmakondu https://orcid.org/0000-0002-7505-077X

William Tiznado https://orcid.org/0000-0002-6061-8879

REFERENCES

[1] W. Siebert, A. Gunale, *Chem. Soc. Rev.* **1999**, *28*, 367.
[2] R. Keese, *Chem. Rev.* **2006**, *106*, 4787.
[3] G. Merino, M. A. Méndez-Rojas, A. Vela, T. Heine, *J. Comput. Chem.* **2007**, *28*, 362.
[4] O. Yañez, A. Vásquez-Espinal, R. Pino-Rios, F. Ferraro, S. Pan, E. Osorio, G. Merino, W. Tiznado, *Chem. Commun.* **2017**, *53*, 12112.
[5] O. Yañez, A. Vásquez-Espinal, R. Báez-Grez, W. A. Rabanal-León, E. Osorio, L. Ruiz, W. Tiznado, *N. J. Chem.* **2019**, *43*, 6781.
[6] H. J. Monkhorst, *Chem. Commun.* **1968**, *18*, 1111.
[7] R. Hoffmann, R. W. Alder, C. F. Wilcox, *J. Am. Chem. Soc.* **1970**, *92*, 4992.
[8] G. Erker, *Inorg. Chem.* **1992**, *13*, 111.
[9] D. Röttger, G. Erker, *Angew. Chem., Int. Ed.* **1997**, *36*, 812.
[10] X. Zhang, Y. Ding, *Comput. Theor. Chem.* **2014**, *1048*, 18.
[11] X. Li, H. Zhang, L. Wang, G. D. Geske, A. I. Boldyrev, *Angew. Chem., Int. Ed.* **2000**, *39*, 3630.
[12] J. Xu, X. Zhang, S. Yu, Y. Ding, K. H. Bowen, *J. Phys. Chem. Lett.* **2017**, *8*, 2263.
[13] C.-J. Zhang, P. Wang, X.-L. Xu, H.-G. Xu, W.-J. Zheng, *Phys. Chem. Chem. Phys.* **2021**, *23*, 1967.
[14] Z.-X. Wang, P. von Ragué Schleyer, *Science* **1979**, *2001*(292), 2465.
[15] Y. Wang, F. Li, Y. Li, Z. Chen, *Nat. Commun.* **2016**, *7*, 11488.
[16] S. Pan, J. L. Cabellos, M. Orozco-Ic, P. K. Chattaraj, L. Zhao, G. Merino, *Phys. Chem. Chem. Phys.* **2018**, *20*, 12350.
[17] Y. Pei, W. An, K. Ito, P. v. R. Schleyer, X. C. Zeng, *J. Am. Chem. Soc.* **2008**, *130*, 10394.
[18] V. Vassilev-Galindo, S. Pan, K. J. Donald, G. Merino, *Nat. Rev. Chem.* **2018**, *2*, 114.
[19] R. Grande-Aztatzi, J. L. Cabellos, R. Islas, I. Infante, J. M. Mercero, A. Restrepo, G. Merino, *Phys. Chem. Chem. Phys.* **2015**, *17*, 4620.
[20] X.-F. Zhao, J.-H. Bian, F. Huang, C. Yuan, Q. Wang, P. Liu, D. Li, X. Wang, Y.-B. Wu, *RSC Adv.* **2018**, *8*, 36521.
[21] Z. Cui, V. Vassilev-Galindo, J. L. Cabellos, E. Osorio, M. Orozco, S. Pan, Y. Ding, G. Merino, *Chem. Commun.* **2017**, *53*, 138.
[22] O. Yañez, R. Báez-Grez, J. Garza, S. Pan, J. Barroso, A. Vásquez-Espinal, G. Merino, W. Tiznado, *ChemPhysChem* **2020**, *21*, 145.
[23] W. Tiznado, L. Leyva-Parra, L. Diego, D. Inostroza, O. Yañez, R. Pumachagua-Huertas, J. Barroso, A. Vásquez-Espinal, G. Merino, *Chem. A Eur. J.* **2021**, *27*, 16701.
[24] Y.-B. Wu, Y. Duan, G. Lu, H.-G. Lu, P. Yang, P. von Rague Schleyer, G. Merino, R. Islas, Z.-X. Wang, *Phys. Chem. Chem. Phys.* **2012**, *14*, 14760.
[25] K. Exner, P. von Ragué Schleyer, *Science* **1979**, *2000*(290), 1937.
[26] L. L. Parra, L. Diego, O. Yañez, D. Inostroza, J. Barroso, A. V. Espinal, G. Merino, W. Tiznado, *Angew. Chem., Int. Ed.* **2021**, *60*, 8700.
[27] Y. Li, Y. Liao, Z. Chen, *Am. Ethnol.* **2014**, *126*, 7376.
[28] L. Yang, E. Ganz, Z. Chen, Z. Wang, P. v. R. Schleyer, *Angew. Chem. Int. Ed* **2015**, *54*, 9468.
[29] L. Leyva-Parra, D. Inostroza, O. Yañez, J. C. Cruz, J. Garza, V. García, W. Tiznado, *Atoms* **2022**, *10*.
[30] N. Perez, T. Heine, R. Barthel, G. Seifert, A. Vela, M. A. Mendez-Rojas, G. Merino, *Org. Lett.* **2005**, *7*, 1509.
[31] N. Perez-Peralta, M. Sanchez, J. Martin-Polo, R. Islas, A. Vela, G. Merino, *J. Org. Chem.* **2008**, *73*, 7037.
[32] P. Das, M. Khatun, A. Anoop, P. K. Chattaraj, *Phys. Chem. Chem. Phys.* **2022**, *24*, 16701.
[33] P. Das, P. K. Chattaraj, *J. Comput. Chem.* **2022**, *43*, 894.
[34] P. Das, P. K. Chattaraj, *Atoms* **2021**, *9*, 65.
[35] J. Cao, G. London, O. Dumele, M. von Wantoch Rekowski, N. Trapp, L. Ruhlmann, C. Boudon, A. Stanger, F. Diederich, *J. Am. Chem. Soc.* **2015**, *137*, 7178.
[36] D. Sundholm, R. J. F. Berger, H. Fliegl, *Phys. Chem. Chem. Phys.* **2016**, *18*, 15934.
[37] J. J. Torres-Vega, A. Vásquez-Espinal, J. Caballero, M. L. Valenzuela, L. Alvarez-Thon, E. Osorio, W. Tiznado, *Inorg. Chem.* **2014**, *53*, 3579.
[38] S. Pelloni, G. Monaco, P. Lazzeretti, R. Zanasi, *Phys. Chem. Chem. Phys.* **2011**, *13*, 20666.

[39] J. J. Torres, R. Islas, E. Osorio, J. G. Harrison, W. Tiznado, G. Merino, *J. Phys. Chem. A* **2013**, *117*, 5529.

[40] C. Foroutan-Nejad, *Theor. Chem. Acc.* **2015**, *134*, 1.

[41] D. Inostroza, V. García, O. Yañez, J. J. Torres-Vega, A. Vásquez-Espinal, R. Pino-Rios, R. Báez-Grez, W. Tiznado, *N. J. Chem.* **2021**, *45*, 8345.

[42] R. Báez-Grez, L. Ruiz, R. Pino-Rios, W. Tiznado, *RSC Adv.* **2018**, *8*, 13446.

[43] F. Feixas, E. Matito, J. Poater, M. Solà, *Chem. Soc. Rev.* **2015**, *44*, 6434.

[44] F. Feixas, E. Matito, J. Poater, M. Solà, *J. Comput. Chem.* **2008**, *29*, 1543.

[45] O. Yañez, R. Báez-Grez, D. Inostroza, W. A. Rabanal-León, R. Pino-Rios, J. Garza, W. Tiznado, *J. Chem. Theory Comput.* **2019**, *15*, 1463.

[46] O. Yañez, D. Inostroza, B. Usuga-Acevedo, A. Vásquez-Espinal, R. Pino-Rios, M. Tabilo-Sepulveda, J. Garza, J. Barroso, G. Merino, W. Tiznado, *Theor. Chem. Acc.* **2020**, *139*, 41.

[47] K. Thirumoorthy, A. L. Cooksy, V. S. Thimmakondu, *Phys. Chem. Chem. Phys.* **2020**, *22*, 5865.

[48] V. S. Thimmakondu, A. Sinjari, D. Inostroza, P. Vairaprakash, K. Thirumoorthy, S. Roy, A. Anoop, W. Tiznado, *Phys. Chem. Chem. Phys.* **2022**, *24*, 11680.

[49] C. Adamo, V. Barone, *J. Chem. Phys.* **1999**, *110*, 6158.

[50] P. Fuentealba, L. Von Szentpaly, H. Preuss, H. Stoll, *J. Phys. B: At. Mol. Phys.* **1985**, *18*, 1287.

[51] S. Grimme, J. Antony, S. Ehrlich, H. Krieg, *J. Chem. Phys.* **2010**, *132*, 154104.

[52] F. Weigend, R. Ahlrichs, *Phys. Chem. Chem. Phys.* **2005**, *7*, 3297.

[53] M. J. Frisch, G. W. Trucks, H. B. Schlegel, G. E. Scuseria, M. A. Robb, J. R. Cheeseman, G. Scalmani, V. Barone, G. A. Petersson, et al. Gaussian 16, Revision B.01. Gaussian, Inc. Wallingford CT, **2016**.

[54] H. Fliegl, S. Taubert, O. Lehtonen, D. Sundholm, *Phys. Chem. Chem. Phys.* **2011**, *13*, 20500.

[55] J. Jusélius, D. Sundholm, J. Gauss, *J. Chem. Phys.* **2004**, *121*, 3952.

[56] K. Wolinski, J. F. Hinton, P. Pulay, *J. Am. Chem. Soc.* **1990**, *112*, 8251.

[57] J. Ahrens, B. Geveci, C. Law, *The Visualization Handbook* **2005**, Cambridge, Massachusetts, p. 717.

[58] U. Ayachit, *The ParaView Guide: A Parallel Visualization Application*, Kitware, Inc, USA **2015**.

[59] M. Abramowitz, *Handbook of Mathematical Functions, With Formulas, Graphs, and Mathematical Tables*, Dover Publications, Inc, New York, NY, USA **1974**.

[60] D. Sundholm, H. Fliegl, R. J. F. Berger, *Wiley Interdiscip. Rev. Comput. Mol. Sci.* **2016**, *6*, 639.

[61] K. B. Wiberg, *Tetrahedron* **1968**, *24*, 1083.

[62] A. E. Reed, R. B. Weinstock, F. Weinhold, *J. Chem. Phys.* **1985**, *83*, 735.

[63] D. Y. Zubarev, A. I. Boldyrev, *Phys. Chem. Chem. Phys.* **2008**, *10*, 5207.

[64] D. Y. Zubarev, A. I. Boldyrev, *J. Org. Chem.* **2008**, *73*, 9251.

[65] E. D. Glendening, J. K. Badenhoop, A. E. Reed, J. E. Carpenter, J. A. Bohmann, C. M. Morales, C. R. Landis, F. Weinhold, *Theoretical Chemistry Institute*, University of Wisconsin, Madison, WI **2013**.

[66] T. Lu, F. Chen, *J. Comput. Chem.* **2012**, *33*, 580.

[67] C. Y. Legault, CYLview, Version 2.0. Université de Sherbrooke, Quebec, Canada. **2020** (http://www.cylview.org)

[68] W. Humphrey, A. Dalke, K. Schulten, *J. Mol. Graph.* **1996**, *14*, 33.

[69] J. M. Millam, V. Bakken, W. Chen, W. L. Hase, H. B. Schlegel, *J. Chem. Phys.* **1999**, *111*, 3800.

[70] S. Seritan, C. Bannwarth, B. S. Fales, E. G. Hohenstein, C. M. Isborn, S. I. L. Kokkila-Schumacher, X. Li, F. Liu, N. Luehr, J. W. Snyder Jr., C. Song, A. V. Titov, I. S. Ufimtsev, L.-P. Wang, T. J. Martínez, *WIREs Comput. Mol. Sci.* **2021**, *11*, e1494.

[71] O. Yañez, A. Vásquez-Espinal, R. Pino-Rios, F. Ferraro, S. Pan, E. Osorio, G. Merino, W. Tiznado, *Chem. Commun.* **2019**, *55*, 12721.

[72] J. J. Torres-Vega, D. R. Alcoba, O. B. Oña, A. Vásquez-Espinal, R. Báez-Grez, L. Lain, A. Torre, V. García, W. Tiznado, *Chemistry (Easton)* **2021**, *3*, 1101.

[73] T. H. Dunning Jr., *J. Chem. Phys.* **1989**, *90*, 1007.

[74] D. E. Woon, T. H. Dunning Jr., *J. Chem. Phys.* **1993**, *98*, 1358.

[75] R. A. Kendall, T. H. Dunning Jr., R. J. Harrison, *J. Chem. Phys.* **1992**, *96*, 6796.

[76] A. K. Wilson, T. van Mourik, T. H. Dunning Jr., *J. Mol. Struct.: THEOCHEM* **1996**, *388*, 339.

[77] J.-D. Chai, M. Head-Gordon, *Phys. Chem. Chem. Phys.* **2008**, *10*, 6615.

SUPPORTING INFORMATION

Additional supporting information can be found online in the Supporting Information section at the end of this article.